Article

Reversible Light-Driven Structural Changes between the Mono- and Bilayer Stacking Alignments in 4-Octadecyloxystilbazolium Arylcarboxylate Films

Osamu Ohtani, Hiroki Kato, Tatsuto Yui, and Katsuhiko Takagi

J. Am. Chem. Soc., **2003**, 125 (47), 14465-14472• DOI: 10.1021/ja030310s • Publication Date (Web): 31 October 2003

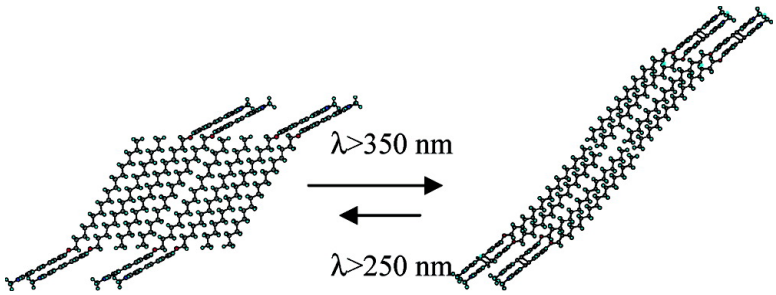

More About This Article

Additional resources and features associated with this article are available within the HTML version:

- Supporting Information
- Access to high resolution figures
- Links to articles and content related to this article
- Copyright permission to reproduce figures and/or text from this article

View the Full Text HTML

J|A|C|S
ARTICLES
Published on Web 10/31/2003

Reversible Light-Driven Structural Changes between the Mono- and Bilayer Stacking Alignments in 4-Octadecyloxystilbazolium Arylcarboxylate Films

Osamu Ohtani,[†] Hiroki Kato,[†] Tatsuto Yui,[†,‡] and Katsuhiko Takagi*[,†]

Contribution from the Department of Crystalline Materials Science, School of Engineering, Nagoya University, Chikusa, Nagoya 464-8603, Japan and CREST (JST)

Received May 21, 2003; E-mail: ktakagi@apchem.nagoya-u.ac.jp

Abstract: The present investigation deals with the light-driven morphological changes in multilamella films of *N*-methyl-4-octadecyloxystilbazolium arylcarboxylates ($C_{18}OStz^+X^-$) cast on glass slides. The results of XRD analysis show a photostimulated layer expansion and shrinkage of the stacked thin films along the *c*-axis under alternative illumination at >350 and 254 nm, respectively. It was revealed that such lamellar changes could be switched either way by a reversible transformation between the mono- and bilayer units in these stacked multilamella films. Moreover, such controlled structural adjustments in the alignment could be initiated by the photocyclodimerization of the stilbazolium moieties of the arylcarboxylate salts; i.e., a monolayer-to-bilayer transformation could be induced at a stage of only 10% cyclodimer formation. The photoinduced patterning on the surface of the films was also analyzed by SEM and fluorescence microscopic investigations.

Introduction

Much interest has recently been focused on photochemically functional devices composed of light-responsive materials in organic supramolecular matrixes.[1] Along these lines, Langmuir−Blodgett (LB) membranes as well as micelles and vesicles have been used as the potent hosts able to organize ionic organic materials in self-assembling multilayer films on glass slides.[2]

There have been a number of works dealing with the morphological changes which can be induced in self-assembling materials by their surrounding physicochemical driving forces.[3−6] Many studies of the *E*−*Z* photochemical isomerization of azobenzenes have been carried out to investigate the morphological changes seen in organic solid matrixes. The polymer matrixes covalently bonded by the azobenzene units have been noted to undergo morphological changes,[4] and a structural reversibility has also been observed between the bilayer and amorphous layers in such self-assembling hydrogen-bonded azobenzene under UV illumination.[7,8]

We have previously reported that structural changes in 1:1 ion-pair composite bilayer films consisting of dioctadecyldimethylammonium bromide and cinnamic acid take place not only in dispersion but also when cast on glass slides, and that such changes can be induced by a photochemical *E*−*Z* photoisomerization and/or a [2+2] photocycloaddition of the cinnamate regions.[9−15] These self-assembling structures have been revealed to be variable with the photochemical transformations of the component olefins.

Although we have briefly communicated an example of the controlled conformational reversibility in cast films of *N*-methyl-4-octadecyloxystilbazolium isophthalate ($C_{18}OStz^+X^-$; X^- = 1,3-benzenedicarboxylate),[14] the present paper is a comprehensive summary of our further detailed investigations into the photoinduced reversible multilayer conformational changes induced in the cast film of $C_{18}OStz^+X^-$ (Chart 1) by photochemical [2+2] cyclodimerization and cycloreversion upon UV light irradiation. Such a control over the properties of the stacking alignment in these thin films can be considered significant for its potential in the design of photofunctional materials.

Experimental Section

Materials. A. 4-Octadecyloxy-*N*-methylstilbazolium Salts ($C_{18}OStz^+X^-$). *n*-Octadecyl bromide, 4-hydroxybenzaldehyde, methyl iodide, 4-methylpyridine, and 1,2-, 1,3-, and 1,4-benenedicarboxylic

[†] Nagoya University.
[‡] CREST.

(1) Fukuda, K.; Nakahara, H.; Shibasaki, Y. *The Chemistry of Supra Thin Molecular Organized Film*; Kodan-sha: Tokyo, 1993.
(2) Shimomura, M. *Immobiled Bilayer Membrane*; Bunshin-sha: Tokyo, 1990; pp 96−136.
(3) Sommerdijk, N. A. J. M.; Booy, K. J.; Pistorius, A. M. A.; Feiters, M. C.; Nolteand, R. J. M.; Zwanenburg, B. *Langmuir* **1999**, *15*, 7008.
(4) Jonas, U.; Shah, K.; Norvez, S.; Charrych, D. H. *J. Am. Chem. Soc*. **1999**, *121*, 4580
(5) Aoki, K.; Nakagawa, M.; Ichimura, K. *J. Am. Chem. Soc*. **2000**, *122*, 10997.
(6) Seki, T.; Fukuda, K.; Ichimura, K. *Langmur* **1999**, *15*, 5098.
(7) Seki, T.; Ichimura, K. *Thin Solid Films* **1989**, *179*, 77.
(8) Tamaoki, N. *Angew. Chem. Int. Ed*. **2001**, *40*, 1135.
(9) Takagi, K.; Itoh, M.; Usami, H.; Imae, T.; Sawaki, Y. *J. Chem. Soc., Perkin Trans*. **1994**, 1003.
(10) Takagi, K.; Sawaki, Y. *Chem. Lett*. **1993**, 2103.
(11) Nakamura, T.; Takagi, K.; Fujita, K.; Katsu, H.; Itoh, M.; Imae, T.; Sawaki, Y. *J. Chem. Soc., Perkin Trans*. **1997**, *2*, 2751.
(12) Takagi, K.; Nakamura, T.; Katsu, H.; Itoh, M.; Sawaki, Y.; Imae, T. *Mol. Cryst. Liq. Cryst*. **1996**, *277*, 135.
(13) Takagi, K.; Aoshima, K.; Sawaki, Y. *J. Am. Chem. Soc*. **1985**, *107*, 47.
(14) Ohtani, O.; Kato, H.; Takagi, K. *Chem. Lett*. **2002**, 49.
(15) Ohtani, O.; Sasai, R.; Adachi, T.; Takagi, K.; Hatta, I. *Langmuir* **2002**, *16*, 1165.

Chart 1. Ion Pairs of $C_{18}OStz^+X^-$ Including the Varying X^-

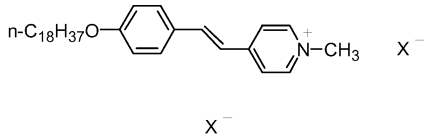

X^-

ClO_4^-

Perchlorate

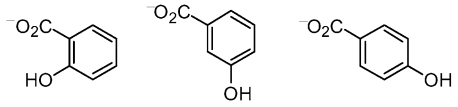

2-Hydroxybenzoate **3-Hydroxybenzoate** **4-Hydroxybenzoate**

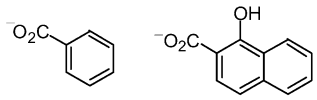

Benzoate **1-Hydroxy-2-naphthoate**

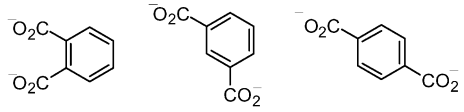

1,2-Benzene dicarboxylate **1,3-Benzene dicarboxylate** **1,4-Benzene dicarboxylate**

Table 1. Product Distributions of the $C_{18}OStz^+X^-$ Films after Irradiation at >350 nm

X^-	irradiatn time/h	selectivity/mol % trans	cis	*syn* HH	*anti* HH
perchlorate	2	85	15	0	0
	10	81	19	0	0
2-hydroxybenzoate	2	53	32	0	15
3-hydroxybenzoate	2	82	13	0	5
	6	69	19	0	12
4-hydroxybenzoate	2	78	22	0	0
	15	63	37	0	0
benzoate	2	73	13	0	14
1-hydroxy-2-naphthoate	2	71	29	0	0
1,2-benzenedicarboxylate	1	53	21	13	13
1,3-benzenedicarboxylate	1	40	32	13	15
1,4-benzenedicarboxylate	1	62	21	8	9

acids of extra pure grade were purchased from Tokyo Kasei Co. Ltd. 4-*n*-Octadecyloxybenzaldehyde was obtained by mixing *n*-octadecyl bromide (40 mmol) with 4-hydroxybenzaldehyde (40 mmol) and anhydrous potassium carbonate (42 mmol) in 300 mL of dry acetone. After the mixture was heated under reflux for 36 h, the product was obtained by extraction with hexane and purification by recrystallization in hexane. 4-[2-(4-*n*-Octadecyloxy)phenylethenyl]pyridine ($C_{18}OStz$) was obtained by heating a mixture of 4-*n*-octadecyloxybenzaldehyde (6.34 mmol) with 4-methylpyridine (19 mmol) in acetic anhydride (20 mmol) under reflux for 16 h. A number of quaternary salts (Table 1) were synthesized as follows.

1. Iodide. The iodide was obtained by mixing $C_{18}OStz$ with methyl iodide (20 mmol) in 30 mL of benzene. The resulting pale yellow solid powder was purified by silica gel column chromatography using hexane and benzene (1:3 v/v), and recrystallized with hexane. Yield: 99%. Mp: 209−212 °C (lit.[16] >200 °C). ^{1}H NMR (δ, 200 MHz, $CDCl_3$): 0.87 (3H, t, Me, J = 6.3 Hz), 1.25 (34H, m, CH_2), 4.01 (2H, t, OCH_2, J = 6.3 Hz), 4.54 (3H, s, *N*-Me), 6.95 (2H, d, aromatic protons, J = 8.6 Hz), 7.00 (1H, d, olefin, J = 16.0 Hz), 7.69 (2H, d, aromatic protons, J = 9.0 Hz), 7.65 (1H, d, olefin, J = 16.0 Hz), 7.94 (2H, d, pyridinium protons, J = 7.0 Hz), 8.90 (2H, d, pyridinium protons, J = 7.2 Hz). UV−vis (MeOH): λ_{max} 385 nm (ϵ = 25000).

2. Perchlorate (X^- = ClO_4^-). The iodide salt $C_{18}OStz^+I^-$ (11.4 mg) dissolved in methanol (20 mL) was added to excess amounts of a saturated aqueous solution of sodium perchlorate to give a yellow precipitate by filtration after condensation of the solvent. Yield: 75%. Mp: 150−158 °C. ESI-MS: m/e = 464 (rel intens 100, M − ClO_4^-).

3. Carboxylates. In addition to the iodide and perchlorate salts, aromatic carboxylate salts of $C_{18}OStz$ were obtained by substituting $C_{18}OStz^+I^-$ with the corresponding sodium aromatic carboxylates in aqueous MeOH.

a. Benzoate. Yield: quantitative. Mp: 96 °C dec.

b. 2-Hydroxybenzoate. Yield: 76%. Mp: 113−115 °C. ^{1}H NMR (δ, Varian INOVA 500 MHz spectrometer, $CDCl_3$): 0.88 (3H, t, Me, J = 7.5 Hz), 6.83 (2H, d, aromatic proton, J = 8.0 Hz), 6.93 (1H, d, olefin, J = 15.5 Hz), 6.95 (1H, d, aromatic proton, J = 9.0 Hz), 7.21 (1H, d, olefin, J = 7.0 Hz), 7.55 (1H, d, aromatic proton, J = 7.5 Hz), 7.57 (1H, d, olefin, J = 16.5 Hz), 7.81 (2H, d, aromatic protons, J = 6.5 Hz), 7.94 (2H, d, pyridinium protons, J = 7.5 Hz), 9.89 (2H, d, pyridinium protons, J = 7.5 Hz). ESI-MS: m/e = 464 (rel intens 100, M − $C_7H_5O_3^-$).

c. 3-Hydroxybenzoate. Yield: 92%. Mp: 93 °C dec.

d. 4-Hydroxybenzoate. Yield: 75%. Mp: 92 °C dec.

e. 1-Hydroxy-2-naphthoate. Yield: 80%. Mp: 122−124 °C.

f. 1,2-Benzenedicarboxylate. Yield: 95%. Mp: 105−107 °C.

g. 1,3-Benzenedicarboxylate. Yield: 96%. Mp: 129−132 °C. ^{1}H NMR (δ, Varian INOVA 500 MHz spectrometer, CD_3OD): 0.89 (6H, t, Me, J = 7.0 Hz), 1.28 (68H, m, CH_2), 4.04 (4H, t, OCH_2, J = 6.5 Hz), 4.27 (6H, s, *N*-Me), 7.00 (4H, d, aromatic protons, J = 9.0 Hz), 7.24 (2H, d, olefin, J = 16.0 Hz), 7.33 (1H, t, protons at the 5-position of isophthalic acid, J = 7.5 Hz), 7.69 (4H, d, aromatic protons, J = 8.5 Hz), 7.87 (2H, d, olefin, J = 16.5 Hz), 7.97 (2H, q, protons at the 4- and 6-positions of isophthalic acid, J = 7.5, 2.0 Hz), 8.07 (4H, d, pyridinium protons, J = 7.0 Hz), 8.61 (1H, t, proton at the 2-position of isophthalic acid, J = 2.0 Hz), 8.63 (4H, d, pyridinium protons, J = 7.0 Hz). ESI-MS: m/e = 464 (rel intens 100, M − $C_8H_5O_4^{2-}$).

h. 1,4-Benzenedicarboxylate. Yield: quantitative. Mp: 124−125 °C.

B. *syn* and *anti* Head-to-Head Cyclodimers of $MeOStz^+X^-$ Salts. *syn* and *anti* head-to-head cyclodimers (HH dimers) as well as the *syn* head-to-tail cyclodimer (HT dimer) of 4-methoxy-*N*-methylstilbazolium ions ($MeOStz^+$) were prepared by irradiation of the AOT (sodium bis(2-ethylhexyl)sulfosuccinate) salt of MeOStz. Irradiation of a 1 L hexane solution of the AOT salt of MeOStz was carried out by a high-pressure Hg lamp for 16 h through a 10% KNO_3 solution (>350 nm). Here, the AOT salt of MeOStz was obtained by extraction with hexane from a mixture of $MeOStz^+Cl^-$ (488.5 mg) in H_2O with AOT (2.06 g) in CH_2Cl_2. After hydrolysis with 6 N HCl (70 mL) followed by neutralization by 1 N NaOH, the photolyzed mixture was separated on a SiO_2 column with acetone−ethyl acetate (1:1 v/v) as the eluent to yield the starting monomers (R_f = 0.41), *syn* HT dimer (R_f = 0.28), *anti* HH dimer (R_f = 0.41), and *syn* HH dimers (R_f = 0.08) as free bases in this order. The obtained cyclodimers were then methylated under reflux with excess amounts of methyl iodide in benzene to obtain yellow precipitates. The characterization data are as follows. ^{1}H NMR (δ, 200 MHz, $CDCl_3$): (*syn* HH) 3.70 (6H, s, MeO), 4.29 (6H, s, *N*-Me), 4.66 (2H, d, cyclobutane protons, J = 7.0 Hz), 5.06 (2H, d, cyclobutane protons, J = 7.2 Hz), 6.75 (4H, d, aromatic

(16) Lupo, D.; Scheunemann, U.; Ringsdorfs, H.; Ledoux, I. *J. Opt. Soc. Am. B* **1988**, *5*, 300.

protons, $J = 8.8$ Hz), 7.14 (4H, d, aromatic protons, $J = 8.8$ Hz), 8.00 (4H, d, pyridinium protons, $J = 7.0$ Hz), 8.69 (4H, d, pyridinium protons, $J = 6.8$ Hz); (*anti* HH) 3.90 (6H, s, MeO), 4.34 (6H, s, *N*-Me), 4.01 (2H, d, cyclobutane protons, $J = 9.2$ Hz), 4.14 (2H, d, cyclobutane protons, $J = 9.0$ Hz), 6.96 (4H, d, aromatic protons, $J = 8.6$ Hz), 7.47 (4H, d, aromatic protons, $J = 8.6$ Hz), 8.00 (4H, d, pyridinium protons, $J = 6.8$ Hz), 8.77 (4H, d, pyridinium protons, $J = 7.0$ Hz); (*syn* HT) 3.70 (6H, s, MeO), 4.26 (6H, s, *N*-Me), 4.98 (4H, t, cyclobutane protons), 6.79 (4H, d, aromatic protons, $J = 8.6$ Hz), 7.39 (4H, d, aromatic protons, $J = 8.8$ Hz), 8.00 (4H, d, pyridinium protons, $J = 6.8$ Hz), 8.65 (4H, d, pyridinium protons, $J = 6.6$ Hz).

C. *syn Head-to-Head* Cyclodimers of $C_{18}OStz^+X^-$ Salts. The *syn* HH cyclodimers of *N*-hydrogen 4-*n*-octadecyloxystilbazolium chloride were prepared by irradiating a 60 mL aqueous solution of this chloride obtained by treating the free base $C_{18}OStz$ (50.6 mg) with 10 mL of 0.6 N HCl. Irradiation was carried out by a high-pressure Hg lamp for 16 h through a 10% KNO_3 solution (>350 nm) under an Ar atmosphere. The photolyzed mixture was neutralized by 1 N NaOH, extracted with $CHCl_3$, and then separated on a SiO_2 column eluted with acetone−benzene (1:1 v/v) to yield the starting monomers ($R_f = 0.58$) and *syn* HH dimers ($R_f = 0.33$). The resulting HH dimers were then methylated with excess amounts of methyl iodide under reflux for 2 h to yield the corresponding iodide. Detailed data are as follows. ^{1}H NMR (δ, 200 MHz, $CDCl_3$): 0.90 (6H, t, Me), 1.30 (68H, m, CH_2), 3.89 (4H, t, OCH_2), 4.34 (3H, s, *N*-Me), 5.10 (2H, d, cyclobutane protons), 6.74 (4H, d, aromatic protons, $J = 8.6$ Hz), 7.12 (4H, d, aromatic protons, $J = 8.6$ Hz), 8.04 (4H, d, pyridinium protons, $J = 7.0$ Hz), 8.77 (4H, d, pyridinium protons, $J = 6.8$ Hz). ESI-MS: $m/e = 464$ (rel intens100, dication), 928 (rel intens <20, monocation).

D. (*Z*)-C_{18}OStz Salts. The *Z*-isomer (*cis*-isomer) of 4-*n*-octadecyloxy-*N*-methylstilbazolium bromide ((*Z*)-$C_{18}OStz^+Br^-$) was prepared in a diluted chloroform solution (ca. 10^{-4} M) by >310 nm light irradiation for 24 h. ^{1}H NMR (δ, Varian INOVA 500 MHz spectrometer, $CDCl_3$): 0.87 (3H, t, Me, $J = 6.3$ Hz), 1.25 (34H, m, CH_2), 3.97 (2H, t, OCH_2, $J = 6.5$), 4.62 (3H, s, *N*-Me), 6.46 (1H, d, olefin, $J = 12.0$ Hz), 6.85 (2H, d, aromatic protons, $J = 9.0$ Hz), 7.06 (1H, d, olefin, $J = 12.0$ Hz), 7.18 (2H, d, aromatic protons, $J = 9.0$ Hz), 7.74 (2H, d, pyridinium protons, $J = 6.5$ Hz), 9.00 (2H, d, pyridinium protons, $J = 7.0$ Hz). ESI-MS: $m/e = 464$ (rel intens 100, M − Br^-).

Measurements. X-ray diffraction analysis was carried out with a RINT 2000 diffractometer (Rigaku) using Cu Kα radiation, operating at 40 kV and 40 mA as the applied voltage and current, respectively. The ultraviolet−visible (UV−vis) absorption spectra were recorded on JASCO (type V-550) and Shimadzu (type UV-265) spectrophotometers. The polarized infrared (IR) and ultraviolet (UV) absorption spectra were recorded on a Hitachi FT-IR spectrophotometer with a polarized unit attachment and a JASCO V-500 spectrophotometer with a JASCO polarizer unit attachment, respectively. The ^{1}HNMR spectra were obtained in $CDCl_3$ using TMS as an internal standard reference sample by a Varian Gemini 200 MHz FT spectrometer (unless otherwise specified).

Preparation of the Films. A. Cast Films. A 0.3 mM solution of $C_{18}OStz^+X^-$ in 10% aqueous methanol was cast on a silica glass slide to give a transparent thin film by heating in a water bath at 60 °C for a few hours and subsequently cooling to 20 °C.

B. LB Membranes. A sample solution was prepared by dissolving several milligrams of $C_{18}OStz^+X^-$ in 0.5 mL of ethanol, which was then diluted to 5 mL by adding chloroform. The resulting chloroform solution was gently developed using a 50 μL microsyringe on the surface of water placed in a Teflon-coated trough of an LB membrane apparatus from the Nippon Laser Electronics Corp. (type NL-BIO20). The pressure−area (π−A) isotherm profiles were taken with the evaporation of the solvents after the solutions stood for 30 min under a ventilated atmosphere.

Irradiation of the Films. The films (20 mm × 20 mm × 1 μm in length, width, and thickness, respectively) were developed on a Pyrex glass plate of 5 mm thickness and irradiated from the film surface at an ambient temperature of around 20 °C, in turns, with light of λ > 350 nm through a filter of aqueous 10% potassium nitrate with a 300 W medium-pressure Hg lamp and by $\lambda = 250.5$ nm light with a xenon lamp of a FP-750 fluorescence spectrophotometer equipped with a monochromator.

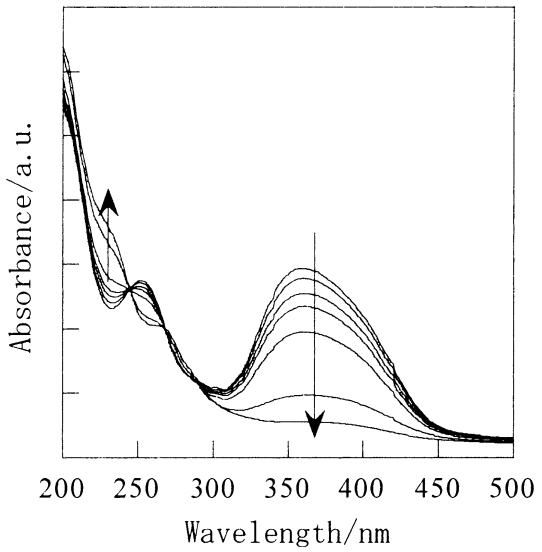

Figure 1. Changes in the absorption spectra of the cast film of $C_{18}OStz^+X^-$ ($X^- = C_6H_5CO_2^-$) under UV irradiation for 2 h.

Results and Discussion

Photolysis of the Thin Films of $C_{18}OStz^+X^-$. Irradiation of the $C_{18}OStz^+X^-$ thin films with light of >350 nm was continued until the disappearance of its absorbance intensities at 350−400 nm. Figure 1 shows the spectral changes observed in the $C_{18}OStz^+X^-$ thin films during light irradiation, clearly indicating the consumption of the olefins with the passing of the irradiation time. After the reaction, the products were extracted from the photolyzed thin films by immersion in a 1:1 (v/v) methanol−acetone mixed solvent, while the reaction mixture was analyzed by ^{1}NMR after condensation in vacuo.

Table 1 summarizes the dependence of the product distribution on the type of counterion, X^-, in the photolysis of the $C_{18}OStz^+X^-$ thin films. Photochemical [2+2] cyclodimerizations in matrixes such as micelles, membranes, or crystals have been reported to take place stereospecifically through an excited singlet state.[9−12] In such cases, a strong excimer fluorescence could be observed. In a similar manner, the $C_{18}OStz^+X^-$ films emit a strong excimer emission for X^- = benzoate and 2- and 3-hydroxybenzoates in which considerable amounts of cyclodimers were formed, while little or nil for X^- = perchlorate, 1-hydroxy-2-naphthoate, and 4-hydroxybenzoate. It can, thus, be assumed that an excimer is preferably formed in the aggregated alignment of stilbazolium ions in these thin films. In fact, $C_{18}OStz^+X^-$ with 1- and 2-hydroxybenzoates as X^- have been reported to form an antiparallel packing structure,[17−19] as shown in Scheme 1. Moreover, the molecular packing of $C_{18}OStz^+$ sandwiched by the X^- anions shows a preferable formation of HH dimers, which is in good correspondence with the stereochemistry shown in Table 1. Table 1 also shows that

(17) Iyer, R. M. *J. Chem. Soc., Chem. Commun.* **1986**, 379.
(18) Bijima, K.; Engberts, J. B. F. N. *Langmuir* **1997**, *13*, 4846.
(19) Bijima, K.; Engberts, J. B. F. N. *Langmuir* **1998**, *14*, 79.

Table 2. (001) Diffraction Angles and the Lamella Distances of the Octadecyloxystilbazolium Salts $C_{18}OStz^+X^-$

X^-	2θ/deg	lamella unit distance/nm	X^-	2θ/deg	lamella unit distance/nm
perchlorate	3.26	2.7	1-hydroxy-2-naphthoate	2.83	3.1
2-hydroxybenzoate	2.6	3.4	1,2-benzenedicarboxylate	2.24	3.9
3-hydroxybenzoate	2.22	3.9	1,3-benzenedicarboxylate	2.57	3.3
4-hydroxybenzoate	2.25	3.9	1,4-benzenedicarboxylate	2.15	4.1
benzoate	2.65	3.3			

Scheme 1. A Model of the Aggregated Structure of $C_{18}OStz^+X^-$ Leading to the Formation of *syn* HH and *anti* HH Dimers

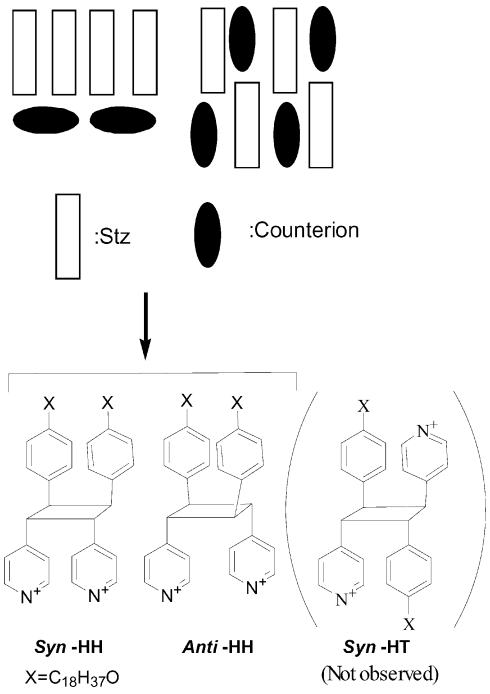

the *syn* HH dimers as well as the *anti* HH dimers are almost equally formed with 1,2-, 1,3-, and 1,4- benzenedicarboxylates as the counterions (X^-), which indicates that the packing conformation is sensitive to the structure of the X^- anions. In contrast, $C_{18}OStz^+X^-$ with perchlorate as X^- may be loosely dissociated due to the rather poor hydrophobicity in which the only observable photochemical reaction is the *E*−*Z* isomerization.

Characterization of the Packing Structure of the $C_{18}OStz^+X^-$ Film. The XRD diffraction patterns are shown in Figure 2, and the (001) diffraction angles are summarized in Table 2 along with the lamella unit distances (*d*). These values indicate the high regularity of the lamella stacking, judging from the fact that higher diffraction peaks of up to the fifth order could be observed.

The lamella unit spaces of 2.7−4.1 nm, which depend on the type of X^-, could be seen to correspond to the distance between the mono- and bilayers for $C_{18}OStz^+X^-$. It is, thus, important to determine the tilt angles of the packed ion pairs in the films to gain a clear understanding of the lamella structure.

Polarized spectroscopies[20−23] were carried out to estimate the tilt angles, γ, of the ion pairs which were calculated by eq 1.

$$R_{yx} = A_y/A_x = \frac{2[\sin^2\theta + (\sin^2\alpha)(3\cos^2(\theta - 1))] - [3\sin^2(\alpha - 1)][3\cos^2(\theta - 1)]\sin^2\gamma}{2\sin^2\theta + (2 - 3\sin^2\theta)]\sin^2\gamma} \quad (1)$$

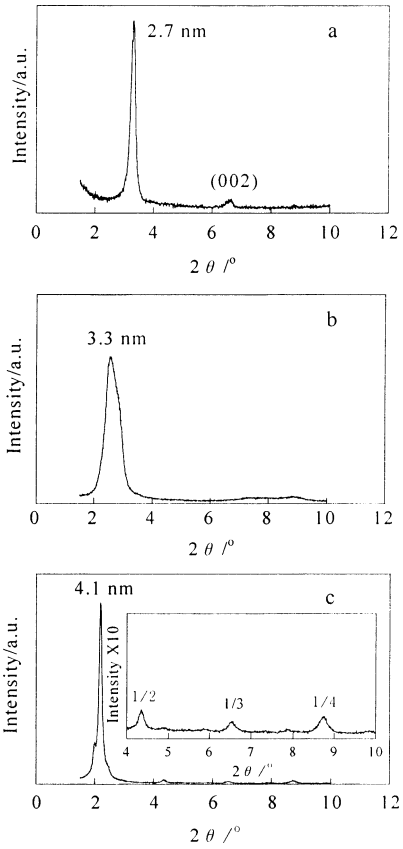

Figure 2. X-ray diffraction profiles of $C_{18}OStz^+X^-$: (a) perchlorate ($X^- = ClO_4^-$), (b) benzoate ($X^- = C_6H_5CO_2^-$), (c) 1,4-benzenedicarboxylate [$X^- = 1,4\text{-}C_6H_4(CO_2^-)_2$].

The ion pairs $C_{18}OStz^+X^-$ possess both a $\pi-\pi^*$ transition of the stilbazolium chromophore at 350−390 nm in the UV region and C−H stretching vibrations of the *all-trans* configurational alkyl chain at 2917 cm^{-1} in the IR region. These characteristic UV and IR absorption peaks were utilized for an estimation of the tilt angles for each chromophore by means of polarized UV and IR spectroscopies, and are compiled in Table 3. The tilt angles of the stilbazolium and alkyl chain moieties arrive at their corresponding values depending on the bulkiness or structure of X^-.

On the basis of the estimation that the stilbazolium ions and alkyl chain of $C_{18}OStz^+X^-$ tilt at around 58° and 32° against the normal line, respectively, $C_{18}OStz^+X^-$ was found to form an antiparallel interdigitated monolayer with the alkyl chains regularly overlapping with those of the adjacent molecules, thus

(20) Akutsu, H.; Kyogoku, Y.; Nakahara, H.; Fukuda, K. *Chem. Phys. Lipids* **1975**, *15*, 222.
(21) Michl, J.; Thulstrup, E. W. *Spectroscopy with Polarized Light*; VHC: New York, 2000.
(22) Sonobe, K.; Kikuta, K.; Takagi, K. *Chem. Mater.* **1999**, *11*, 4.
(23) Sasai, R.; Ogiso, H.; Shindachi, I.; Shichi, T.; Takagi, K. *Tetrahedron* **2000**, *56*, 6979.

Table 3. Tilt Angles of the Stilbazolium and Polymethylene Parts of $C_{18}OStz^+X^-$ Normal to the Silica Substrate of the Cast Film

X^-	$\gamma^{stilbazolium}$	$\gamma^{polymethylene}$	X^-	$\gamma^{stilbazolium}$	$\gamma^{polymethylene}$
perchlorate	68	42	1-hydroxy-2-naphthoate	58	38
2-hydroxybenzoate	58	38	1,2-benzenedicarboxylate	54	29
3-hydroxybenzoate	52	29	1,3-benzenedicarboxylate	58	32
4-hydroxybenzoate	54	30	1,4-benzenedicarboxylate	51	30
benzoate	58	34			

indicating the parallel aggregation of the stilbazolium moieties to those of the surrounding ion pairs.

***π*−*A* Isothermal Profile Measurements.** To gauge the effect of the counterion of the ion pair on the correlation between the photochemical behavior and morphological characteristics, observations of the $\pi-A$ curve were carried out to provide useful information on the solubilization site. Hydrophobic counterions such as salicylate or isophthalate ions can be solubilized by the stilbazolium ions within the adjacent molecules due to favorable hydrophobic interactions, whereas hydrophilic counterions such as perchlorate ions are not able to penetrate into the aggregated stilbazolium molecules. The $\pi-A$ isothermal profile was measured by developing monolayer membranes of a series of $C_{18}OStz^+X^-$ on the surface of by using an LB membrane apparatus, as shown in Figure 3. The cross-section of the $C_{18}OStz^+X^-$ molecules was estimated to be ca. 0.33 nm^2 at a surface pressure of 0 mN/m for X^- = perchlorate, which is comparable to the value of 0.35 nm^2 for X^- = iodide.[18] On the other hand, $C_{18}OStz^+X^-$ molecules with hydrophobic counterions such as arylcarboxylates had cross-sections of 0.4−0.6 nm^2 for their polar headgroups.

The perchlorate ion-pair is assumed to be perpendicularly oriented on the substrate on the basis of Chem 3D calculations which showed the cross-section of the ion pair to be 0.35 nm^2. On the other hand, $C_{18}OStz^+X^-$ molecules with hydrophobic counterions, such as arylcarboxylates, possess larger cross-sections of around 0.4−0.6 nm^2 for their polar headgroups due to the intimate interaction of the counterions with the cationic headgroups. This is understood by the assumption that the hydrophilic perchlorate ion pair is easily hydrated and dissociates at the stage of compression during $\pi-A$ measurements, whereas the arylcarboxylate ion pairs are easily sandwiched between the hydrophobic stilbazolium aggregates.

Indeed, the pressure from the collapse of the arylcarboxylate ion pair monolayers tends to be lower than that for the perchlorate ion pair monolayers. This is explicable by the fact that the headgroups of the arylcarboxylate ion pair are bulkier than those of the perchlorate ion pair, and as a result, the monolayer films consisting of arylcarboxylate are considered to be more fragile than those of perchlorate.

Photoinduced Morphological Changes in the Cast Films. The photoinduced morphological changes which can be induced in these self-assembling cast films may be developed for applications in the design of photofunctional materials capable of reversible memory storage.[3−6] Ogawa et al. have reported the changes observed in the basal spacings triggered by the $E-Z$ photoisomerization of the azobenzene chromophores in organophilic clay−azobenzene intercalation compounds.[24]

To verify the origin of the structural changes observed in these cast films upon light irradiation, the correlation between the efficiency of the photochemistry and the structural changes has been studied in films of such stilbazolium salts, i.e., for perchlorate and isophthalate ($C_{18}OStz^+isoph^-$). And, in fact,

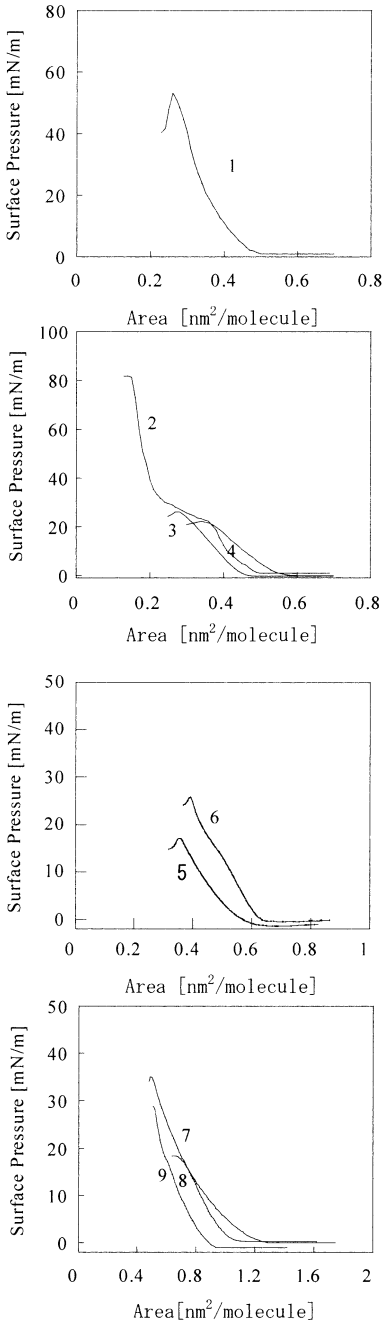

Figure 3. $\pi-A$ isotherm of $C_{18}OStz^+X^-$: (1) perchlorate ($X^- = ClO_4^-$), (2) 2-hydroxybenzoate [$X^- = 2\text{-}C_6H_5(OH)CO_2^-$], (3) 3-hydroxybenzoate [$X^- = 3\text{-}C_6H_5(OH)CO_2^-$], (4) 4-hydroxybenzoate [$X^- = 4\text{-}C_6H_5(OH)CO_2^-$], (5) benzoate ($X^- = C_6H_5CO_2^-$), (6) 1-hydroxy-2-naphthoate [$X^- = 1,2\text{-}C_{10}H_6(OH)CO_2^-$], (7) 1,2-benzenedicarboxylate [$X^- = 1,2\text{-}C_6H_4(CO_2^-)_2$], (8) 1,3-benzenedicarboxylate [$X^- = 1,3\text{-}C_6H_4(CO_2^-)_2$], (9) 1,4-benzenedicarboxylate [$X^- = 1,4\text{-}C_6H_4(CO_2^-)_2$].

(24) Ogawa, M.; Fujii, K.; Kuroda, K.; Kato, C. Mater. *Res. Soc. Symp. Proc.* **1991**, *233*, 89.

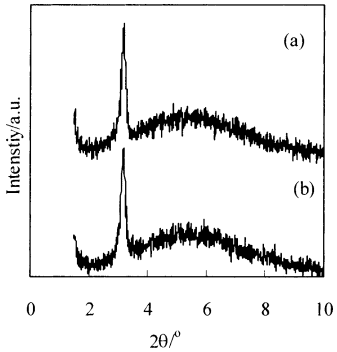

Figure 4. Changes in the X-ray diffraction patterns of perchlorate $C_{18}OStz^+ClO_4^-$ (a) before and (b) after irradiation at >350 nm.

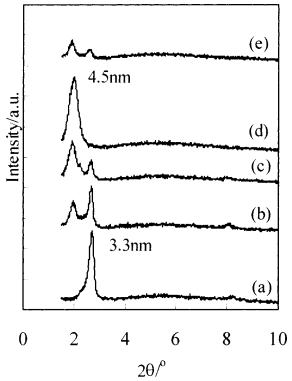

Figure 5. X-ray diffraction changes in the isophthalate $C_{18}OStz^+X^-$ [$X^- = 1,3\text{-}C_6H_4(CO_2^-)_2$] upon irradiation at >350 nm: (a) 0 min, (b) 15 min, (c) 30 min, (d) 1 h. Pattern (e) shows a mixture of *syn* HH and $C_{18}OStz^+isoph^-$ in a molar ratio of 0.02.

two divergent reaction pathways, i.e., $E-Z$ isomerization and/or [2+2] cyclodimerization, could be observed upon light irradiation of these stilbazolium salts. Moreover, our studies showed that only the *Z*-isomer was formed in the case of perchlorate, while both the *Z*-isomer and *anti* HH dimers could be seen for isophthalate.

Figure 4 shows the X-ray profiles for the perchlorate before and after irradiation at >350 nm. As the isomerization progressed to form a *Z*-isomer, little change in the intensity of the X-ray diffraction peak of the starting perchlorate (*E*-isomer) could be observed. The present *E*-to-*Z* isomerization could not induce lamella structural changes along the *c*-axis, most probably due to the fact that the molecular length of the *Z*-isomer of perchlorate is essentially the same as that for the *E*-isomer.

In contrast, the X-ray profiles measured for the isophthalate ($C_{18}OStz^+isoph^-$) film before and after irradiation at >350 nm show that the structural changes observed for $C_{18}OStz^+isoph^-$ were different from those of the perchlorate film, as shown in Figure 5. That is, in the case of photodimerization, the reflection peaks (001) of the starting film decreased with an increase in the new peaks (001) at a lower angle of about $2\theta = 2°$, in stark contrast to the case of only $E-Z$ photoisomerization.

Here, a control experiment was undertaken to estimate the amount of dimer content necessary to induce a structural change from mono- to bilayer in the lamella of the films. An estimated content percentage of the HH dimers, from 0 to 10%, was dissolved in aqueous $C_{18}OStz^+isoph^-$ solution, cast onto the glass slide, and then analyzed by XRD.

With an increase in the percentage of the HH dimers in the mixture**,** new peaks (001) appeared at a lower angle of around

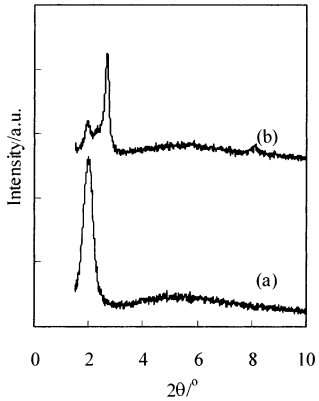

Figure 6. X-ray diffraction changes in the isophthalate $C_{18}OStz^+X^-$ [$X^- = 1,3\text{-}C_6H_4(CO_2^-)_2$] (a) before and (b) after irradiation at >250 nm.

Table 4. Change of the Tilt Angles of the Stilbazolium and Polymethylene Parts of $C_{18}OStz^+X^-$ in the Cast Films before and after Irradiation at >350 nm

X^-	$\gamma^{stilbazolium}$	$\gamma^{polymethylene}$
before irradiation	58	32
after irradiation	55	47

$2\theta = 2°$, and only 10% HH dimers was confirmed to be sufficient in inducing a complete transformation into a bilayer lamellar structure, which can be observed by the change into completely new peaks, as can be seen in XRD pattern e of Figure 5. These new peaks showed a good correspondence with those for the photolyzed films.

Photocycloreversion. Stilbazolium ion dimers are capable of undergoing photochemical cycloreversions. In fact, photolysis of *N*-methylstilbazolium methyl sulfate dimers at 254 nm in water reverted these dimers to the original stilbazolium salts with an efficiency in the order *syn* HH < *syn* HT < *anti* HH dimer ions.[25] Similar photochemical cycloreversions of $C_{18}OStz^+isoph^-$ may take place in the thin films containing the *syn* HH dimers formed by photodimerization upon irradiation of 254 nm light to generate the starting $C_{18}OStz^+isoph^-$. The olefins were formed with a yield of 15% after 2 days of irradiation at 254 nm. Along with the cycloreversion, the resulting thin film was observed to lose its characteristic bilayer structure and to regenerate the peak at 3.3 nm, as shown in Figure 6. Moreover, around 50% recovery of the photoinduced morphological change could be observed by direct irradiation at 254 nm.

Changes in the Molecular Angle against the SiO_2 Glass Surface. To determine the tilt angles of polymethylene in the $C_{18}OStz^+isoph^-$ film, the R_{yx} ratio was calculated from the absorbance intensity at 2916 cm^{-1} and plotted against the angle α. Both of the R_{yx} values of the films before and after 2 h of irradiation were plotted against the angle α. The values of the angle γ, calculated from eq 1, are compiled in Table 4. The values of the angle γ of the component polymethylene chains against the normal line on the substrate in the irradiated films were found to be larger than those of the nonirradiated samples, indicating the greater tilt of the polymethylene chain in the irradiated, as-prepared samples than for the nonirradiated samples.

(25) Nakamura, T.; Takagi, K.; Sawaki, Y. *Bull. Chem. Soc. Jpn.* **1998**, *71*, 419.

Scheme 2. Reversible Changes Seen in the Self-Assembling Structure of $C_{18}OStz^+isoph^-$ upon Irradiation: (a) Interdigitated Monolayer, (b) Bilayer Structure

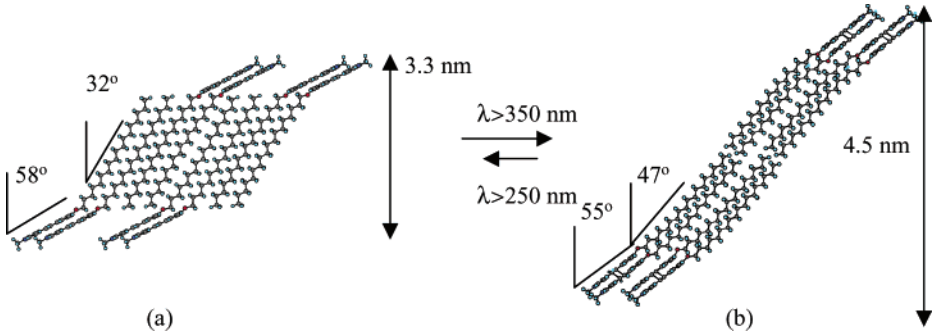

Cyclodimerization, and not the $E-Z$ photoisomerization, is assumed to be the crucial driving force behind the origin of the morphological changes in the ion pair film of the stilbazolium ions during UV light irradiation. This is verified by an experiment showing no difference in the lamella unit distances before and after *E*-to-*Z* photoisomerization of the perchlorate ion pair. Additionally, XRD analysis showed no changes in the lamella unit distance of the ion pair film of the *Z*-isomer, whereas the stilbazolium ion pair film including 10% *syn* head-to-head cyclodimers was observed to exhibit a lamella distance 1.5 times larger than that of the original stilbazolium ion pair film. It is understood that a [2+2] cycloaddition of the adjacent two stilbazolium ions worked to drive out the alkyl chains of the oppositely oriented stilbazolium ion pairs to induce morphological changes from an interdigitated monolayer to a bilayer packing morphology, as is described in the following section.

Structural Elucidation by X-ray Diffraction and Polarized Spectroscopies. The lamella structure of the $C_{18}OStz^+isoph^-$ film was clearly characterized to be tilted against the normal line on the substrate, as shown from estimations of the lamella unit length and electron density distribution of the ion pair films, as depicted in Scheme 2. XRD analysis indicated that the lamella unit distance of 3.3 nm corresponds exactly to the value (3.3 nm) of the interdigitated monolayer of the $C_{18}OStz^+isoph^-$ molecules in the nonirradiated film (Scheme 2a), when the lengths of the stilbazolium and octadecyloxy moieties are 1.0 and 2.6 nm, respectively. Hydrophobic counterions, such as these aromatic carboxylates, can hardly be dissolved or diffused in the water bulk and, hence, are easily and preferably solubilized with the hydrophobic stilbazolium ions. Here, a bilayer structure could be depicted so as to fit the lamella units having a distance of 4.5 nm, as shown in Scheme 2b. Moreover, the stilbazolium groups were seen to be bulkier and more tilted than the octadecyloxy moieties.

The electron density distribution of the two morphologies, i.e., interdigitated monolayer and bilayer, was estimated by using higher reflection signals for the XRD analysis. The interdigitated monolayer structure could be clearly confirmed by electron density distribution analysis using a series of XRD peaks up to the fifth-order reflection; however, the bilayer structure exhibited no peaks higher than the second-order reflection, so it could not be estimated.

SEM Images. The surface of the $C_{18}OStz^+isoph^-$ thin films on the SiO_2 glass plate was analyzed by means of a scanning electron microscope. UV irradiation of the $C_{18}OStz^+isoph^-$ thin films at >350 nm through a photomask resulted in the appearance of definite and clear patterns after 1 h of irradiation,

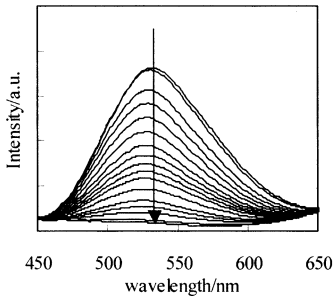

Figure 7. Changes observed in the fluorescence intensities of $C_{18}OStz^+isoph^-$ upon UV irradiation for 1 h.

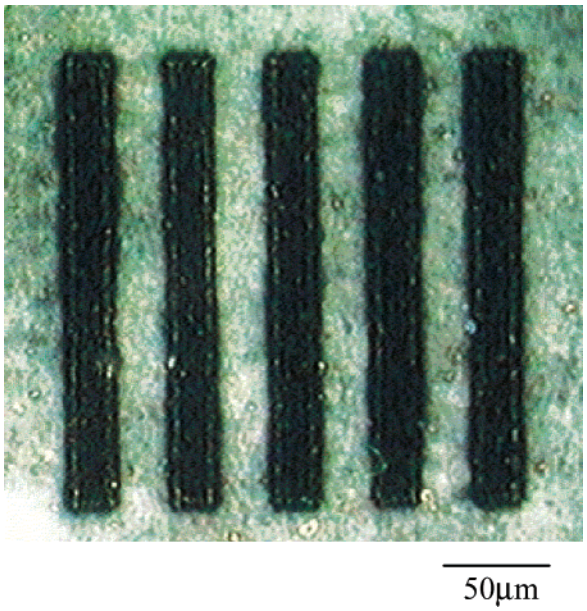

Figure 8. Fluorescence images of the $C_{18}OStz^+isoph^-$ patterns.

together with the formation of some cracks in the patterns. In contrast, the perchlorate salt $C_{18}OStz^+ClO_4^-$ exhibited no patterns even after UV irradiation under similar conditions. Patterning of the lamella unit can be explained by the generation of cyclodimers which induced a larger expansion of the lamella unit in the course of the photochemical [2+2] cycloaddition, a crucial factor in clear patterning formation.

Fluorescence Microscopy. The images of the patterns can also be observed using fluorescence microscopy excited at around 350 nm. Figure 7 shows the successive changes of the fluorescence intensities of the $C_{18}OStz^+isoph^-$ thin films while undergoing photocyclodimerization upon UV irradiation at 350 nm.

Figure 8 shows the black and white images excited by the fluorescence intensities of the $C_{18}OStz^+isoph^-$ thin film at 350 nm. In the patterning, the bright and white zone was observed to emit a strong fluorescence at around 520 nm.

Conclusions

Fluorescence and UV−vis spectroscopies, NMR analysis, and $\pi-A$ isotherm investigations have revealed a correlation between the photochemical behavior and the packing structure of stilbazolium salts $C_{18}OStz^+X^-$ in thin films cast on SiO_2 glass plates. Photocyclodimerization was found to be a crucial factor in initiating structural changes in the morphology of the $C_{18}OStz^+X^-$ films. Significantly, the alignment of the $C_{18}OStz^+X^-$ self-assembly in the cast films could be well controlled by the kinds of counterions of the salts. Moreover, analyses of the X-ray diffraction patterns and polarized IR/UV−vis spectroscopy showed that UV irradiation at >350 nm induces a dramatic change from interdigitated monolayer units to partial bilayer units in the lamella structure of the solid films. Such controlled structural changes in organic compounds initiated by photocyclodimerization shows great potential for applications in the design of photofunctional and erasable recording materials.

Acknowledgment. This work was partly supported by a Grant-in Aid for Scientific Research on Priority Areas (417) of the Ministry of Education, Science, Culture, and Sports, Science and Technology (MEXT), of Japan. Thanks are also extended to CREST (Core Research for Evolutional Science and Technology) of JST (Japan Science and Technology Corp.) for their kind support.

Supporting Information Available: XRD profiles of a mixture of HH dimers and $C_{18}OStz^+isoph^-$, relationship between R_{yx} and α of $C_{18}OStz^+isoph^-$ films on SiO_2 solid glass, and SEM images of the $C_{18}OStz^+isoph^-$ patterns (PDF). This material is available free of charge via the Internet at http://pubs.acs.org.

JA030310S